Overcoming Chromatic-Dispersion Effects in Fiber-Wireless Systems Incorporating External Modulators

Graham H. Smith, *Student Member, IEEE*, Dalma Novak, *Member, IEEE*, and Zaheer Ahmed

***Abstract*—We demonstrate two techniques to reduce the effects of fiber chromatic dispersion in fiber-wireless systems incorporating external modulators. We theoretically and experimentally show that the achievable link distance can be increased by varying the chirp parameter of the modulator to give large negative chirp using a dual-electrode Mach–Zehnder modulator (MZM) biased at quadrature. In addition, we show that dispersion can be almost totally overcome by implementing a simple method using the dual-electrode MZM to generate an optical carrier with single sideband (SSB) modulation. We demonstrate the transmission of a 51.8-Mb/s pseudorandom bit sequence (PRBS) at 12 GHz over 80 km of standard single-mode fiber using the SSB generator and measure a bit-error-rate (BER) power penalty due to fiber dispersion of less than 0.5 dB for a BER equal to 10^{-9}.**

***Index Terms*— Millimeter-wave generation, optical-fiber communication, optical-fiber dispersion.**

I. Introduction

BROAD-BAND wireless access is a promising technology to provide future interactive multimedia services. Wireless connectivity to a network can provide quick and cheap installation for a large number of closely spaced customers. In such systems, the RF signals can be generated at a local exchange using optical techniques and distributed to remote antenna sites using optical fiber links, which provide large bandwidth, low loss, and immunity to EMI. This distribution system also enables small, simple, and cheap base stations to be implemented.

Several methods have been reported for the generation of modulated RF optical carriers in fiber-wireless systems. These include optical heterodyne [1] and self-heterodyne techniques [2], and fundamental and harmonic signal generation using pulsed lasers [3], [4]. However, the simplest technique for the optical generation and distribution of the RF signal modulated with data is an intensity modulation scheme via direct or external modulation of a laser. Since direct modulation suffers from the effects of laser frequency chirps externally modulated optical fiber links are the preferred choice.

In conventional intensity modulation, the optical carrier is modulated to generate an optical field with the carrier and two sidebands (double-sideband (DSB) modulation). At the optical receiver, each sideband beats with the optical carrier, thereby generating two beat signals which constructively interfere to produce a single component at the RF frequency. However, if the signal is transmitted over fiber, chromatic dispersion causes each spectral component to experience different phase shifts depending on the fiber-link distance, modulation frequency, and the fiber-dispersion parameter. These phase shifts result in relative phase differences between the carrier and each sideband, and produce a phase difference in the two beat signals at the RF frequency, which results in a power degradation of the composite RF signal [5]. When the phase difference is π, complete cancellation of the RF signal occurs. As the RF frequency increases, the effect of dispersion is even more pronounced and the fiber-link distance severely limited [6]–[8].

In this paper, we theoretically and experimentally show that dispersion effects can be reduced and fiber-link distances improved by using an external modulator with a negative chirp. Such a Mach–Zehnder modulator (MZM) has two electrodes which can be independently driven so as to vary the chirp parameter of the modulator [9]. In particular, we show that by making the chirp large and negative, it is possible to almost double the achievable fiber-link distance for a certain wireless frequency. We also show that dispersion effects can be reduced further and almost totally overcome by eliminating one sideband to produce an optical carrier with single-sideband (SSB) modulation. Optical SSB has been previously demonstrated with baseband digital transmission to overcome fiber dispersion, whereby an optical filter was used to suppress one of the sidebands [10]. However, this technique can be complex to implement and is limited by the filter characteristics. Here we outline a novel technique which requires no optical filtering and uses only a single dual-electrode modulator biased at quadrature to generate optical SSB and overcome the effects of dispersion in fiber-wireless systems. We demonstrate the transmission of a 51.8-Mb/s pseudorandom bit sequence (PRBS) on a 12-GHz RF carrier over 80 km of standard single-mode fiber and show with bit-error-rate (BER) measurements a fiber-dispersion penalty of less than 0.5 dB for a BER of 10^{-9}.

Manuscript received November 28, 1996; revised April 19, 1997.

G. H. Smith and D. Novak are with the Australian Photonics Cooperative Research Centre, Photonics Research Laboratory (PRL), Department of Electrical and Electronic Engineering, University of Melbourne, Parkville, Vic. 3052, Australia.

Z. Ahmed was with the Australian Photonics Cooperative Research Centre, Photonics Research Laboratory (PRL), Department of Electrical and Electronic Engineering, University of Melbourne, Parkville, Vic. 3052, Australia. He is now with Philips Public Telecommunications Systems, Melbourne 3170, Australia.

Publisher Item Identifier S 0018-9480(97)06020-1.

II. Dual Electrode MZM and Chromatic-Dispersion Theory

The dual-electrode MZM can be modeled as two phase modulators in parallel, where the amplitudes of the RF drive signals applied to each electrode are equal. A continuous-wave (CW) signal from a laser with amplitude A and frequency f_c is externally modulated by an RF signal with peak-to-peak amplitude $2V_{\rm ac}$ and frequency $f_{\rm rf}$, which is split and applied to each drive electrode. A phase difference of θ can exist between each drive electrode. If the modulator has a dc-bias voltage of $V_{\rm dc}$ on one electrode while the other dc terminal is grounded, then the output optical field is represented by

$$E(t) = \frac{A}{2}\{\cos(\omega_c t + \gamma\pi + \alpha\pi\cos\omega_{\rm rf} t) + \cos(\omega_c t + \alpha\pi\cos[\omega_{\rm rf} t + \theta])\} \quad (1)$$

where $\omega_c = 2\pi f_c$, $\omega_{\rm rf} = 2\pi f_{\rm rf}$, $\gamma = (V_{\rm dc}/V_\pi)$ is the normalized bias voltage, V_π is the switching voltage of the MZM and $\alpha = (V_{\rm ac}/V_\pi)$ is the normalized amplitude of the drive signal. This equation can be expanded in terms of Bessel functions to give

$$\begin{aligned} E(t) = \frac{A}{2}\{&J_0(\alpha\pi)[\cos(\gamma\pi)+1]\cos(\omega_c t) \\ &- J_0(\alpha\pi)\sin(\gamma\pi)\sin(\omega_c t) \\ &- J_1(\alpha\pi)\cos(\gamma\pi)[\sin(\omega_c-\omega_{\rm rf})t \\ &+ \sin(\omega_c+\omega_{\rm rf})t] - J_1(\alpha\pi)\sin(\gamma\pi)[\cos(\omega_c-\omega_{\rm rf})t \\ &+ \cos(\omega_c+\omega_{\rm rf})t] - J_1(\alpha\pi)[\sin\{(\omega_c-\omega_{\rm rf})t-\theta\} \\ &+ \sin\{(\omega_c+\omega_{\rm rf})t+\theta\}] + \cdots\} \end{aligned} \quad (2)$$

where J_0 and J_1 are the zeroth- and first-order Bessel functions, respectively.

When both RF electrodes of the MZM are driven with the same signal and a phase difference of $\theta = \pi$ in one arm, and if the applied dc voltage biases the MZM at quadrature ($\gamma = \frac{\pi}{2}$), then (2) simplifies to

$$\begin{aligned} E(t) = \frac{A}{2}\{&J_0(\alpha\pi)\cos(\omega_c t) - J_0(\alpha\pi)\sin(\omega_c t) \\ &- J_1(\alpha\pi)[\cos(\omega_c-\omega_{\rm rf})t + \cos(\omega_c+\omega_{\rm rf})t] \\ &+ J_1(\alpha\pi)[\sin(\omega_c-\omega_{\rm rf})t + \sin(\omega_c+\omega_{\rm rf})t] \\ &+ \cdots\}. \end{aligned} \quad (3)$$

The Fourier transform of the autocorrelation of $E(t)$ will give the power-spectral density, $S_E(\omega)$:

$$\begin{aligned} S_E(\omega) = \frac{\pi A^2}{4}\big[&J_0^2(\alpha\pi)\delta\{\omega+\omega_c\} \\ &+ J_1^2(\alpha\pi)\delta\{\omega+(\omega_c-\omega_{\rm rf})\} \\ &+ J_1^2(\alpha\pi)\delta\{\omega+(\omega_c+\omega_{\rm rf})\}\big] \end{aligned} \quad (4)$$

where $\delta\{\,\}$ represents a delta function. This spectrum consists of an optical carrier at ω_c, with DSB modulation showing components at $\omega_c - \omega_{\rm rf}$ and $\omega_c + \omega_{\rm rf}$.

In standard single-mode fiber, each optical frequency travels through the fiber at different velocities due to the chromatic-dispersion properties of the fiber. It can be shown that phase changes in the optical sidebands alter the resultant phase of the RF beat signals and the RF power $P_{f_{\rm rf}}$ of the generated radio frequency $f_{\rm rf}$ will vary approximately as

$$P_{f_{\rm rf}} \propto \cos\left[\frac{\pi L D}{c}\lambda_c^2 f_{\rm rf}^2\right] \quad (5)$$

where D is the dispersion parameter, L is the length of the fiber, and λ_c is the carrier wavelength. The argument of the cosine function in (5) indicates that for a fixed radio frequency $f_{\rm rf}$, the fiber lengths at which power cancellation occurs will be given by

$$L = \frac{N\,c}{2D\lambda_c^2 f_{\rm rf}^2}, \qquad N = 1,3,5,\cdots. \quad (6)$$

III. Effect of Modulator Chirp in Fiber-Wireless Systems

The chirp parameter ν is important in externally modulated systems as it indicates the phase of the output signals from the modulator. Equations (5) and (6) assume that the MZM chirp is zero. While MZ interferometer-type intensity modulators can be designed to operate completely chirp-free, in most devices there is a small residual chirp arising from an asymmetry in the overlap of the electric fields at each electrode [11]. A dual-electrode MZM which allows access to both electrodes can be used to achieve a variable chirp parameter. For such a device, the chirp parameter can be related to the relative amplitude and sign of the RF drive signals to each electrode V_1 and V_2 via [11]

$$\nu = \frac{V_1 + V_2}{V_1 - V_2}. \quad (7)$$

A related parameter for a modulator is the α parameter, which represents the ratio of phase to amplitude modulation and is defined by [12]

$$\alpha = \frac{1}{2S}\frac{\left(\frac{d\phi}{dt}\right)}{\left(\frac{dS}{dt}\right)} \quad (8)$$

where φ and S are the instantaneous phase and intensity at the output of the modulator. For an MZM, α is a function of the modulation depth and dc-bias point, and is related to ν via [12]

$$\alpha_{\rm MZ} = \nu\tan\left(\frac{\pi}{2}\frac{V_{\rm dc} - V_o - V_\pi}{V_\pi}\right) \quad (9)$$

where V_o is the offset voltage corresponding to the phase retardation with no applied electric field. Equation (9) indicates that the modulator can be biased to obtain both positive or negative values of $\alpha_{\rm MZ}$ and that if the modulator is biased at quadrature, i.e., $V_{\rm dc} = V_o + V_\pi/2, V_o + 3V_\pi/2, \cdots$, then $|\alpha_{\rm MZ}| = |\nu|$.

In high-speed baseband digital transmission it has been shown that dispersion-induced power penalties can be reduced using a modulator with a small negative chirp [9]. In fiber-wireless systems employing MZM's, dispersion effects will also be influenced by the modulator chirp. Since $\alpha_{\rm MZ}$ affects the phase of the spectral components, it will affect the fiber distance at which the RF beat signals after the photodiode

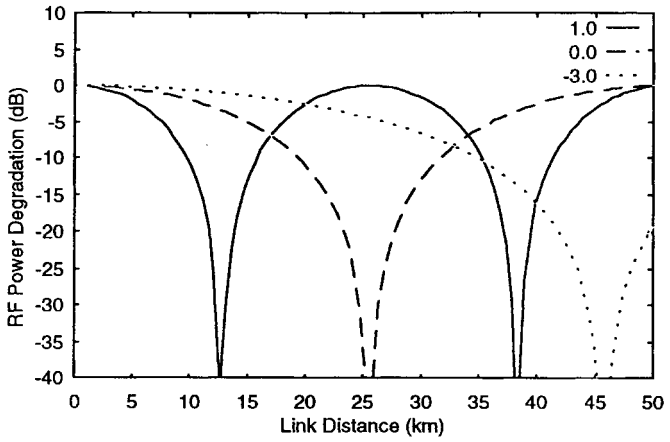

Fig. 1. Calculated degradation of RF power versus fiber transmission distance for several values of α_{MZ} ($f_{\mathrm{rf}} = 12$ GHz).

exhibit a π phase difference. If the MZM has chirp, then (6) can be rewritten as [13]

$$L = \frac{c}{2D\lambda_c^2 f_{\mathrm{rf}N}^2}\left(N - \frac{2}{\pi}\arctan(\alpha_{\mathrm{MZ}})\right), \qquad N = 1, 3, 5, \cdots. \tag{10}$$

Equation (10) indicates that the fiber-link distances in externally modulated analog systems can be increased when α_{MZ} is large and negative. For MZM's which have nonzero chirp, optimum transmission distances can, therefore, be obtained by biasing on the appropriate slope of the MZM transfer function.

A more useful determination of achievable transmission distance is to consider the detected RF power at the modulating frequency Pf_{rf}. Using (5) and (10), $P_{f\mathrm{rf}}$ will be given by

$$P_{f_{\mathrm{rf}}} \propto \cos\left\{\frac{\pi L D \lambda_c^2 f_{\mathrm{rf}}^2}{c\left[1 - \frac{2}{\pi}\arctan(\alpha_{\mathrm{MZ}})\right]}\right\}. \tag{11}$$

We can define an RF power degradation as the difference in the post-detection RF powers before and after transmission through the optical fiber. Fig. 1 shows the predicted RF power degradation due to dispersion as a function of fiber length for various values of α_{MZ} in a 1550-nm optical fiber link externally modulated with a 12-GHz RF signal. It is evident that compared to a modulator having zero chirp ($\nu = 0$ thus $\alpha_{\mathrm{MZ}} = 0$), the fiber-link distance is almost doubled when $\alpha_{\mathrm{MZ}} = -3$.

IV. Generation of SSB Modulation Using the Dual-Electrode MZM

In the previous section, theoretical improvement in optical fiber-link distances was shown by varying the chirp of the MZM, however, the effects of dispersion will still limit the maximum transmission distance. In order to overcome dispersion effects, optical SSB modulation must be implemented. When a phase difference of $\theta = \pm\frac{\pi}{2}$ is applied in the two RF electrodes of the dual-electrode MZM, as shown in Fig. 2, (2) simplifies to

$$E(t) = \frac{A}{2}[J_0(\alpha\pi)\cos\omega_c t - J_0(\alpha\pi)\sin\omega_c t \pm 2J_1(\alpha\pi)\cos(\omega_c \pm \omega_{\mathrm{rf}})t] \tag{12}$$

and the power-spectral density, $S_E(\omega)$ is given by

$$S_E(\omega) = \frac{A^2}{4}J_0^2(\alpha\pi)\pi\delta(\omega + \omega_c) + \frac{A^2}{2}J_1^2(\alpha\pi)\pi\delta(\omega + (\omega_c \pm \omega_{\mathrm{rf}})). \tag{13}$$

The first term in (13) is the optical carrier at wavelength $\lambda_c = 2\pi c/\omega_c$, while the second term represents either a lower or upper sideband at the optical frequencies $\omega_c - \omega_{\mathrm{rf}}$ and $\omega_c + \omega_{\mathrm{rf}}$, respectively.

V. Dual-Electrode MZM with Variable Chirp Experiment

While α_{MZ} can be varied from $-\infty$ to $+\infty$ in all MZ modulators with nonzero chirp by varying V_{dc} [see (9)], operating at the quadrature point enables larger drive levels to be applied to the modulator and also minimizes the generation of harmonics. Therefore, in order to bias the modulator at quadrature and obtain an optimum α_{MZ} for maximum link distance, the chirp parameter ν of the modulator itself should be varied. Experiments were carried out in order to confirm the results predicted in Section III. The effects of dispersion were investigated for two MZM's: a single-electrode device and a dual-electrode variable chirp modulator. A schematic of the experimental setup is shown in Fig. 2. A distributed feedback (DFB) laser with output power -2.0 dBm acts as the optical source for the modulator. V_π for the single electrode modulator was measured as 13.0 V while the dual-electrode device had $V_\pi = 8.2$ V. The optimum operating point was achieved by biasing at quadrature and applying an RF signal with a drive level of 0.45 V_π where the second and higher order harmonic-frequency components were negligible. The RF modulating signal was obtained from a 0-to-20 GHz synthesizer and amplified before being applied to the modulator. The modulated optical signal was then transmitted over 79.6 km of single-mode fiber. To compensate for the 18-dB attenuation loss of the fiber link, the signal was amplified by a low-noise erbium-doped fiber amplifier (EDFA) with a gain of 18 dB. The effects of dispersion were investigated by using a lightwave signal analyzer to measure the RF power degradation as the difference between the detected RF power at 79.6 km and the detected RF power at 0 km. In this way, the effect of the MZM frequency response on the detected RF power was avoided.

Fig. 3 shows the measured RF power degradation as a function of the frequency of the applied RF signal, for the optical link incorporating the single-electrode MZM. As expected, Fig. 3 shows a periodic degradation in the received RF power, with power nulls observed at 6.6, 11.9, 15.7, and 18.0 GHz. Also shown in Fig. 3 is the calculated variation in RF power degradation. In order to determine the chirp parameter for this modulator, a linear regression technique [13] was used to fit the measured frequency nulls to (11). This method predicted a value for D of 17 ps/nm/km and $\alpha_{\mathrm{MZ}} = -0.1$. A negative value of α_{MZ} was expected since the modulator was biased on the negative slope of the transfer characteristic at the quadrature point.

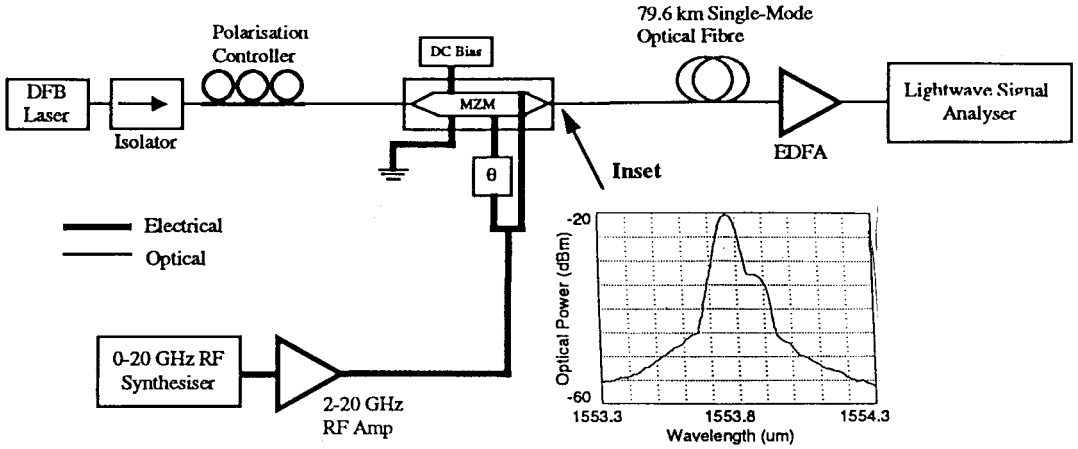

Fig. 2. Experimental setup to measure the effect of fiber chromatic dispersion in externally modulated links and schematic diagram of dual-electrode MZM [inset shows the measured optical spectrum from the optical SSB generator ($f_{\rm rf} = 18$ GHz)].

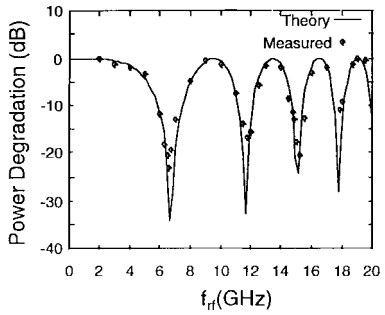

Fig. 3. Measured RF power degradation for single-electrode MZM with $\alpha_{\rm MZ} = -0.1$ after transmission through 79.6 km of single-mode fiber.

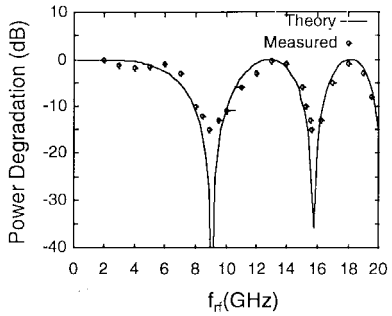

Fig. 4. Measured RF power degradation for dual-electrode MZM with $\alpha_{\rm MZ} = -3.0$ after transmission through 79.6 km of single-mode fiber.

Fig. 4 shows the measured effects of dispersion using the dual-electrode variable-chirp MZM. This modulator was also biased on the negative slope of its transfer characteristic at quadrature. In this experiment, an RF power divider was used to supply signals to both electrodes, and attenuators were used to control the applied voltages. Using (7), the relative amplitudes of the voltages were adjusted to give a chirp parameter of 3. As Fig. 4 shows, the first two RF power nulls occurred at frequencies of 9.1 and 15.8 GHz, significantly higher than those obtained with the single-electrode modulator with $\nu = 0.1$. As before, a linear regression technique was used to determine $\alpha_{\rm MZ}$ with a value of -3.0 predicted. This gave an excellent match to the chirp parameter calculated using (7) and the magnitude of the voltages applied to the electrodes of the modulator.

The experimental results in this section confirm the theory presented in Section III, which predicts that longer transmission distances can be achieved in externally modulated links by using negative-chirp modulators. A dual-electrode MZM with $\alpha_{\rm MZ} = -3$, for example, enables the transmission of a 28-GHz RF carrier over 5 km of fiber for only a 3-dB power degradation in received RF power. Thus, externally modulated links employing variable-chirp modulators are an attractive alternative for fiber-wireless systems and are most practical for systems transporting radio signals at frequencies less than 30 GHz (where commercial modulators are readily available) over shorter link distances.

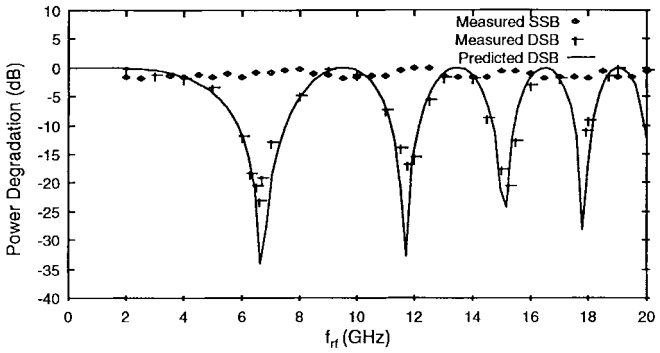

Fig. 5. Measured RF power degradation for optical SSB modulation after transmission through 79.6 km of single-mode fiber.

VI. Optical SSB Generation Experiment

In the previous section, we experimentally showed that optical fiber-link distances could be improved by varying the chirp of the MZM; however, chromatic-dispersion effects will still limit the maximum transmission distance. In order to *overcome* dispersion effects, optical SSB modulation must be implemented. To confirm our theoretical predictions of optical SSB generation from (13), the setup shown in Fig. 2 was implemented with θ set to $\pi/2$. V_π for the modulator was 8.2 V and $V_{\rm dc}$ was 3.9 V, biasing the MZM at quadrature. A 0–20-GHz synthesizer and a 2–20-GHz amplifier provide the RF signals for both MZM electrodes via a 3-dB coupler,

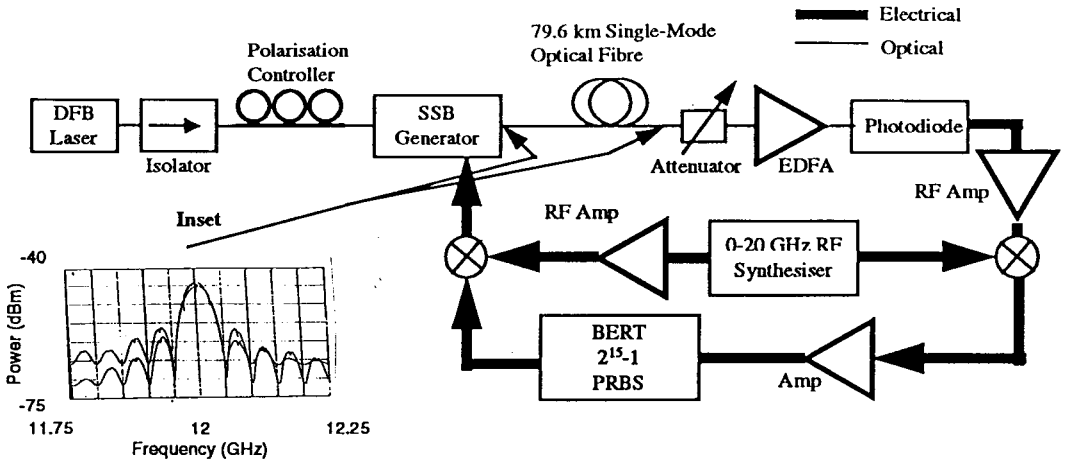

Fig. 6. Experimental setup of 51. 8 Mb/s RF BPSK data transmission at 12 GHz using optical SSB modulation [inset shows the measured RF spectra of 12-GHz BPSK signals at 0 (lower) and 79.6 km (upper)].

with approximately +10-dBm RF power applied to each electrode. At this drive power no second or higher order harmonic components were observed. A broad-band phase shifter provides either of the required $\pm\frac{\pi}{2}$ phase differences in the drive signals. The optical spectrum at the output of the MZM when the drive frequency was 18 GHz was observed on an optical spectrum analyzer with 0.1-nm resolution and is shown in the inset of Fig. 2. Optical SSB is clearly evident, with the power in the upper sideband 13 dB lower than the power in the carrier. For the dual-electrode modulator used in this paper, +10-dBm RF power at each electrode corresponds to a normalized RF input voltage $\alpha\pi$ of approximately 0.36. Using (13) to predict the amplitude difference between the optical carrier and the sideband gives a theoretical value of 12 dB, which is in good agreement with the measured value.

The experimental setup for measuring the effects of fiber dispersion for optical SSB generation was the same as that shown in Fig. 2. The measured RF power degradation due to fiber dispersion as a function of the applied RF frequency is shown in Fig. 5 with a maximum power degradation of 1.5 dB observed for the SSB generator. This is primarily due to experimental error arising from the phase shifter $(\pm\pi/30)$, differences in the applied RF power to the MZM electrodes ($\pm$0.2 dB), and the accuracy in dc bias ($\pm$0.1 V). Including these errors in our model gives a maximum expected power degradation of 2.0 dB. For comparison with the optical SSB generator, Fig. 5 also shows the measured and modeled RF power degradations using the single-electrode MZM (DSB modulation).

We have also demonstrated reduced effects of fiber dispersion when the optical SSB generator is used to transmit an RF signal modulated with data. The experimental setup is shown in Fig. 6. A 51.8 Mb/s, $2^{15}-1$ PRBS derived from the pattern generator of a BER testset (BERT) modulates the phase of a 12-GHz RF carrier in binary phase-shift key (BPSK) format. This RF signal is then applied to both the optical SSB generator and the single-electrode MZM for comparison. Again the output signals from the MZM's were propagated over 79.6 km of single-mode fiber. The RF spectra of the detected 12-GHz BPSK signals at 0 and 79.6 km for

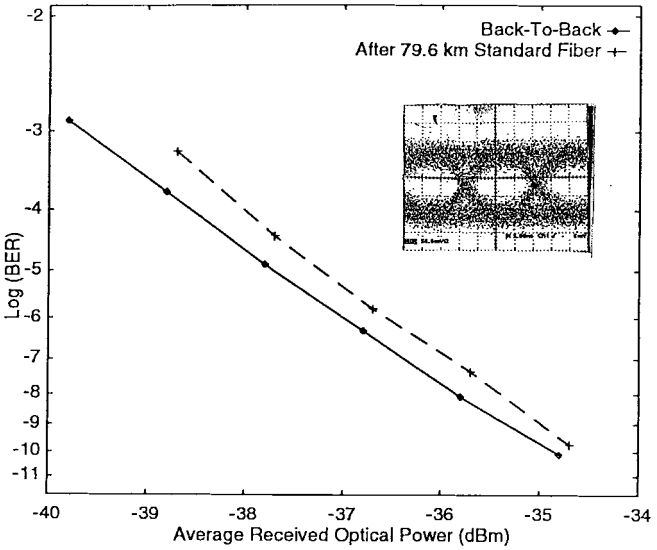

Fig. 7. Measured BER for the recovered BPSK data (inset shows the eye diagram for the received 51.8-Mb/s PRBS).

SSB modulation are shown in the inset of Fig. 6. The slight asymmetry in the signals detected is due to the characteristics of the balanced mixer and the frequency responses of the drive amplifier, phase shifter, and MZM. In the DSB modulation, the 12-GHz BPSK signal suffers the expected RF power degradation of 15 dB when sent over a distance of 79.6 km. Thus, the BPSK data is only recoverable using optical SSB modulation.

The modulated RF signal is amplified and downconverted by coherent detection and directed to the BERT for BER measurements. Fig. 7 compares the measured back-to-back and system BER as a function of the average received optical power. The difference between the back-to-back and system measurement is the 79.6-km fiber link. This fiber link introduced an additional 18-dB insertion loss, so an optical attenuator was inserted to compensate for this. Therefore, only chromatic dispersion is affecting the BER measurement. The plots indicate that the optical SSB system exhibits a power penalty of less than 0.5 dB for a BER of 10^{-9} due to fiber

dispersion. The inset of Fig. 7 shows the eye diagram of the received PRBS at a BER of 10^{-9}.

VII. Conclusion

We have presented a detailed investigation of the impact of fiber chromatic dispersion on link distance in fiber-wireless systems incorporating externally modulated links. Previously reported link distances for fiber-wireless systems have assumed chirp-free MZM's, however in this paper we have shown that the chirp parameter of a modulator will also affect the achievable link distance. By optimizing the chirp parameter, we have demonstrated an increase in link distance which is almost twice that achievable with chirp-free modulators. This method is an attractive technique for fiber-wireless systems transporting radio signals at frequencies where commercial modulators are readily available and where shorter fiber lengths are to be implemented.

To overcome the maximum fiber-link length imposed by fiber dispersion effects in externally modulated systems, we also presented a simple and novel technique for the generation of an optical carrier with SSB modulation. Our method uses a dual-electrode MZM biased at quadrature and driven with signals at the RF electrodes which are $\pi/2$ out of phase. A 1.5-dB degradation in RF power due to fiber dispersion was experimentally observed using optical SSB to distribute 2–20 GHz signals over 79.6 km of single-mode fiber. We also demonstrated data transmission using optical SSB modulation. 51.8-Mb/s BPSK data at 12 GHz was transmitted over 79.6 km of fiber and BER measurements performed. A power penalty due to chromatic dispersion of less than 0.5 dB was measured at a BER of 10^{-9}.

Acknowledgment

The authors thank Dr. J. Archer and CSIRO Telecommunication and Industrial Physics, Sydney, Australia, for their support. The authors also wish to thank Dr. J. Lacey, Dr. G. Pendock, Dr. M. Summerfield, Dr. J. Badcock, and Dr. A. Lowery for useful discussions.

References

[1] G. J. Simonis and K. G. Purchase, "Optical generation, distribution, and control of microwaves using laser heterodyne," *IEEE Trans. Microwave Theory Tech.*, vol. 38, pp. 667–669, May 1990.

[2] D. Wake, C. R. Lima, and P. A. Davies, "Optical generation of millimeter-wave signals for fiber-radio systems using a dual-mode DFB semiconductor laser," *IEEE Trans. Microwave Theory Tech.*, vol. 43, pp. 2270–2276, Sept. 1995.

[3] D. Novak, Z. Ahmed, R. B. Waterhouse, and R. S. Tucker, "Signal generation using pulsed semiconductor lasers for application in millimeter-wave wireless links," *IEEE Trans. Microwave Theory Tech.*, vol. 43, pp. 733–734, Sept. 1995.

[4] D. Kim, M. Pelusi, Z. Ahmed, D. Novak, H.-F. Liu, and Y. Ogawa, "Ultrastable millimeter-wave signal generation using hybrid modelocking of a monolithic DBR laser," *Electron. Lett.*, vol. 31, pp. 733–734, 1995.

[5] G. J. Meslener, "Chromatic dispersion induced distortion of modulated monochromatic light employing direct detection," *IEEE J. Quantum Electron.*, vol. 20, pp. 1208–1216, Oct. 1984.

[6] H. Schmuck, "Comparison of optical millimeter-wave system concepts with regard to chromatic dispersion," *Electron. Lett.*, vol. 31, pp. 1848–1849, 1995.

[7] G. H. Smith, D. Novak, and Z. Ahmed, "Optimization of link distance in fiber-radio systems incorporating external modulators," in *Proc. Australian Conf. Opt. Fiber Technol.*, Gold Coast, Australia, Dec. 1996, pp. 141–144.

[8] U. Gliese, S. Nørskov, and T. N. Nielsen, "Chromatic dispersion in fiber-optic microwave and millimeter-wave links," *IEEE Trans. Microwave Theory Tech.*, vol. 44, pp. 1716–1724, Oct. 1996.

[9] A. H. Gnauck, S. K. Korotky, J. J. Veselka, J. Nagel, C. T. Kemmerer, W. J. Minford, and D. T. Mower, "Dispersion penalty reduction using an optical modulator with adjustable chirp," presented at the *Topical Meeting Integrated Photon. Res.*, Monterrey, CA, Apr. 1991.

[10] K. Yonenaga and N. Takachio, "A fiber chromatic dispersion compensation technique with an optical SSB transmission in optical homodyne detection systems," *IEEE Photon. Technol. Lett.*, vol. 5, pp. 949–951, Aug. 1993.

[11] A. Djupsjobacka, "Residual chirp in integrated-optic modulators," *IEEE Photon. Technol. Lett.*, vol. 4, pp. 41–43, Jan. 1992.

[12] M. Schiess and H. Carlden, "Evaluation of the chirp parameter of a Mach–Zehnder intensity modulator," *Electron. Lett.*, vol. 30, pp. 1524–1525, 1994.

[13] F. Devaux, Y. Sorel, and J. F. Kerdiles, "Simple measurement of fiber dispersion and of chirp parameter of intensity modulated light emitter," *J. Lightwave Technol.*, vol. 11, pp. 1937–1940, Dec. 1993.

Graham H. Smith (S'97) received the Bachelor of Engineering (with honors) and Master of Engineering Science degrees from the University of Queensland, Queensland, Australia, in 1991 and 1993, respectively. In 1996, he began working toward the Ph.D. degree at the Photonics Research Laboratory (PRL), Department of Electrical and Electronic Engineering, University of Melbourne, Parkville, Vic., Australia.

In 1993, he joined the millimeter-wave circuit and systems program at CSIRO Telecommunications and Industrial Physics as a Research Engineer, working in the areas of HEMT modeling, MMIC design (CAD), MMIC packaging, millimeter-wave antenna design, cryogenic systems, measurement systems, and millimeter-wave communication systems. His research interests include electromagnetics, CAD, millimeter-wave MMIC's and packaging, optical generation of millimeter-wave signals, fiber-optic distribution of millimeter-waves, and architectures for millimeter-wave networks.

Dalma Novak (S'90-M'91) received the Bachelor of (Electrical) Engineering (with first-class honors) and the Ph.D. degrees from the University of Queensland, Queensland, Australia, in 1987, and 1992, respectively.

In 1992, she joined the Photonics Research Laboratory (PRL), Department of Electrical and Electronic Engineering, University of Melbourne, Parkville, Vic., Australia, where she is currently a Senior Lecturer and manages the Centre Project on Fiber-Wireless Access Systems. Her research interests include fiber-optic wireless, high-speed optical communication systems and millimeter-wave signal generation using semiconductor lasers.

Dr. Novak is Chair of the IEEE Victorian Section and a member of the Executive Committee of the Australian Chapter of the IEEE Lasers and Electro-optics Society.

Zaheer Ahmed received the B.Sc. degree in electrical engineering from the University of Engineering and Technology, Lahore, Pakistan, in 1989, and the Ph.D. degree from the Photonics Research Laboratory (PRL), University of Melbourne, Parkville, Vic., Australia, in 1996.

From 1989 to 1991, he worked as a Research Engineer at the Carrier Telephone Industries (Pvt.) Ltd., Islamabad, Pakistan. From 1995 to 1996, he was a Research Fellow at PRL, and in 1997 he joined Philips Public Telecommunication Systesm, Melbourne, Australia where he is currently an RF and Optic-Product Manager.